ARTICLES

^{27}Al and ^{19}F Solid-State NMR Studies of Zeolite H-β Dealuminated with Ammonium Hexafluorosilicate

Hsien-Ming Kao* and Yun-Chu Chen

Department of Chemistry, National Central University, Chung-Li, Taiwan 32054

Received: July 19, 2002; In Final Form: December 9, 2002

The dealumination of zeolite H-β by ammonium hexafluorosilicate (i.e., $(NH_4)_2SiF_6$, AHFS) treatment was investigated by ^{27}Al and ^{19}F solid-state NMR, combined with ^{27}Al/^{19}F double resonance NMR. The NMR results demonstrated that the experimental conditions of AHFS dealumination, that is, in the presence and absence of ammonium acetate (NH_4OAc), strongly affected the amount, state, and nature of extraframework aluminum (EFAl) species. Different aluminum fluoro-complexes after dealumination were detected. ^{19}F and ^{27}Al NMR results revealed that the essential part of the dealumination process carried on with AHFS in the presence of NH_4OAc was that most of the extracted Al^{3+} reacted with F^- to form $(NH_4)_3AlF_6$ species that were evident from the signals at 0 ppm in the ^{27}Al spectrum and −143 ppm in the ^{19}F spectrum, respectively. In the absence of NH_4OAc, a resonance at 13 ppm and a broad pattern spread from −20 to −90 ppm in the ^{27}Al spectrum were observed, indicating the presence of two different forms of aluminum fluoro-complexes other than $(NH_4)_3AlF_6$ after dealumination. There were significant differences in their ^{27}Al chemical shifts and spectral line shapes despite the geometry of all these complexes corresponding to a hexacoordination. These aluminum fluoro-complexes showed multiple lines located in the range of −150 to −156 ppm in the ^{19}F spectrum. Discrimination between these different species was made by monitoring the change of ^{19}F peak shift as a function of AHFS content. The correlation between ^{19}F and ^{27}Al spins was also made with the use of double resonance methods such as ^{19}F{^{27}Al} TRAPDOR and ^{27}Al{^{19}F} REDOR NMR. Complementary characterizations with ^{27}Al and ^{19}F NMR as a function of AHFS content have been useful to make peak assignments, and to elucidate possible reaction pathways during AHFS dealumination.

Introduction

An essential step in the preparation of an active, stable zeolite catalyst is the modification of the as-synthesized material. Dealumination, the removal of framework aluminum atoms without severely destroying the micropore structure of zeolites, is an important process that allows adjustments in the Si/Al ratio of zeolites, hence their acidity and catalytic properties. For example, the dealumination of zeolite Y not only improves its hydrothermal stability but also influence its catalytic cracking properties.[1] The nature and strength distribution of acid sites can vary significantly with the aluminum content that can be controlled by the methods of dealumination. Although the dealumination of zeolites is generally carried out through hydrothermal treatment,[2] it can also be accomplished with acid leaching such as HCl,[3] oxalic acid,[4] or critic acid,[5] and with chemical treatments such as silicon tetrachloride[6] or ammonium hexafluorosilicate, $(NH_4)_2SiF_6$ (AHFS).[8] Depending on the methods used for dealumination, acidic properties of zeolites may be enhanced dramatically, often accompanied by a substantial amount of extraframework aluminum (EFAl) formed inside the zeolite structure. Moreover, different zeolite structure types, such as β, mordenite, Y, and ZSM-5, are known to exhibit a very different behavior toward the various dealumination methods.[7] The fluorosilicate method, reported by Skeels and Breck in 1983,[8] has the advantages, in comparison with the other dealumination methods such as thermal or hydrothermal treatments, that silicon atoms can directly replace the extracted aluminum atoms while still maintaining much of the crystallinity of the sample. However, critical choices of the operating conditions have been emphasized.[8,9]

Zeolite β processes a three-dimensional channel system with 12-membered ring apertures of 5.5 × 7.3 Å.[10] Spectroscopic techniques such as FT-IR and multinuclear solid-state NMR have been used as powerful tools for characterization of the composition and acid sites of zeolite β. The state of aluminum species in zeolite β was first studied by Bourgeat-Lami et al. with ^{27}Al magic angle spinning (MAS) NMR.[11] On the basis of IR, and ^{29}Si and ^{27}Al MAS NMR studies, zeolite β has been shown to be very easily dealuminated.[12−14] For example, calcination or steaming above 673 K causes progressive dealumination with deposition of EFAl inside the channels. It was found that the environment of aluminum atoms in the β zeolite framework could be changed from tetrahedral to octahedral upon calcination of an ammonium zeolite, and this change was reversible in the presence of ammonium, pyridine,

* Corresponding Author. Tel: +886-3-4275054. Fax:+886-3-4227664. E-mail: hmkao@cc.ncu.edu.tw.

10.1021/jp021680q CCC: $25.00
Published on Web 03/25/2003

or often ionic exchange.[14] When the compensating cation was H^+, octahedral aluminum was always detected, and "NMR-invisible" aluminum also existed. More recently, Kentgens et al.[15] demonstrated that stepwise dealumination at specific T-positions in the β framework can be monitored using high spinning ^{27}Al MAS and ^{27}Al MQ (multiple quantum) MAS NMR.

Despite extensive dealumination of zeolites by various methods, only a limited number of studies have focused on the dealumination of zeolites with AHFS, since it is a relatively mild agent for dealumination. Besides studies on the nature of the local coordination environment of the aluminum atoms, there has been little effort done to elucidate the nature of the modifications brought about by AHFS treatment. Although possible pathways in the modification of zeolites treated with AHFS were proposed,[8] a full characterization of the state and exact nature of aluminum, and fluorinated species formed during the dealumination process still remains to be determined.

The goal of this work is to address the nature and type of aluminum fluoro-complexes formed during the dealumination process using ^{27}Al and ^{19}F solid-state NMR in an attempt to gain more insight into the dealumination mechanisms induced by AHFS. The reaction scheme can be sketched if the fate of aluminum is monitored, and various forms of fluorides are characterized. Therefore, ^{27}Al MAS NMR is used to monitor the state and exact nature of EFAl species as a function of AHFS content and hydration level of dealuminated samples, and ^{19}F MAS NMR to probe the fluorinated species formed during AHFS dealumination. Double resonance NMR methods, namely ^{19}F{^{27}Al} REDOR (Rotational Echo Double Resonance)[16] and ^{27}Al{^{19}F} TRAPDOR (Transfer Population in Double Resonance)[17] NMR, are employed to help the assignment of ^{19}F NMR peaks, and to make the correlation between ^{27}Al and ^{19}F nuclei. Furthermore, a comparison of the dealumination process in the presence and absence of ammonium acetate (NH_4OAc) has been made to shed light on what happened in the dealumination process.

Experimental Section

Sample Preparation. The parent zeolite used in this study was NH_4-β, obtained from Zeolyst with a Si/Al ratio of 12.5. The dehydrated H-β zeolite was prepared from NH_4-β by slowly ramping the temperature of the sample to 400 °C over a period of 12 h, under vacuum; the sample was kept at this temperature for another 12 h. Dealumination of H-β by AHFS was carried out using a variation of the method of Skeels and Breck.[8] Two series of dealuminated samples were prepared. First, one gram of H-β was preheated at 80 °C in 50 mL of 3.0 M aqueous solution of NH_4OAc. The initial pH of the zeolite solution was approximately 7, and was then lowered to about 6.5 by the dropwise addition of 10 mL of aqueous AHFS solution with various concentrations over a period of 1 h. The solution was then kept at 80 °C with constant stirring for another 3 h. The resulting solution was cooled to room temperature, filtered, and then dried, *without prior washing*, in an oven at 60 °C overnight. In contrast to the standard procedure of AHFS treatment, no additional washing with hot water was done in order to characterize all the EFAl and fluorinated species formed after dealumination. The amount of AHFS was chosen to obtain a molar ratio of AHFS to the total Al of the parent zeolite varying from 0.5 to 6.4. These dealuminated samples were designated as H-β/AHFS-x-NH_4OAc, where x denotes the molar ratio of AHFS to the total Al content of the parent zeolite. It was found that experimental parameters, e.g., pH, were critical on the extent and nature of the dealumination. For comparison, another series of dealuminated samples were prepared using the same procedure without adding NH_4OAc. The final pH of the solution prepared in this way was 4.1. These dealuminated samples were labeled as H-β/AHFS-x-None. X-ray powder patterns of these two series of dealuminated H-β samples, along with the calcined H-β sample, showed that the dealumination via AHFS treatment did not bring any significant change in the crystallinity.

Purely siliceous MCM-41 materials with AHFS treatments were also prepared for ^{19}F NMR measurements in order to make a comparison with dealuminated H-β samples. MCM-41 materials were synthesized following the conventional procedure using sodium silicate and cetyltrimethylammonium bromide as the source materials for silicon and surfactant, respectively.[18] MCM-41 samples were subjected to calcination in air at 560 °C for 6 h to remove the organic templates. The structure of the synthesized material was confirmed by powder X-ray diffraction. The average pore size and BET surface area of the calcined MCM-41 sample, deduced from the adsorption curve of the N_2 adsorption−desorption isotherm obtained at 77 K, were 29.8 Å and 1030 $m^2\ g^{-1}$, respectively.

NMR Measurements. ^{19}F and ^{27}Al NMR spectra were recorded on a Bruker DSX-300 spectrometer equipped with a 4 mm MAS probe with resonance frequencies of 282.23 and 78.17 MHz, respectively. Some ^{27}Al MAS NMR spectra were measured on a Bruker AVANCE-400 spectrometer. All ^{27}Al MAS NMR spectra were obtained with small flip angles of approximately 15° and with a recycle delay of 1 s in order to make a quantitative comparison of the number of ^{27}Al spins.[19] To favor a symmetric environment around the aluminum nucleus, all samples were hydrated under atmospheric moisture conditions for 24 h before acquiring the spectrum. These samples were denoted as partially hydrated samples. To investigate the effect of hydration on the status and nature of aluminum in dealuminated zeolites, partially hydrated samples were further hydrated for a week, which were designated as fully hydrated samples. ^{19}F MAS NMR spectra were acquired with a $\pi/2$ pulse of 4.5 μs and a recycle delay of 15 s, and at a spinning speed of 12 kHz. A Hahn echo sequence was applied for refocusing the magnetization lost in the dead time and the signal distorted by the probe. Several thousand scans were accumulated. The ^{19}F and ^{27}Al chemical shifts were externally referenced to $CFCl_3$ and $Al(H_2O)_6^{3+}$ at 0.0 ppm, respectively.

Simulations of ^{27}Al NMR line shapes were performed with the WINFIT program of the Bruker WINNMR software package to extract both the qradrupole coupling constant (QCC) and the asymmetry parameter (η). Additional interactions such as ^{27}Al−^{19}F dipolar coupling were not taken into account.

^{27}Al{^{19}F} REDOR NMR. In the ^{27}Al{^{19}F} REDOR NMR experiments, the ^{27}Al spins were monitored, and thus short pulses (e.g., 1 and 2 μs for $\pi/2$ and π pulse, respectively) were applied to the ^{27}Al spins, to ensure that the whole solid sample was uniformly excited. The intensities of the ^{27}Al echoes were measured with and without applying a series of ^{19}F π pulses at half integral multiples of the rotor cycles. The expected difference signal, normalized to the full echo intensity, i.e., the REDOR fraction, depends on the strength of the ^{27}Al−^{19}F dipolar coupling and the total dephasing time.[16]

^{19}F{^{27}Al} TRAPDOR NMR. TRAPDOR NMR experiments were used to correlate ^{19}F spins with ^{27}Al spins within the dealuminated zeolite samples. The pulse sequence used in the ^{19}F{^{27}Al} TRAPDOR NMR experiments was similar to those used in ref 17. A comprehensive description of the method with

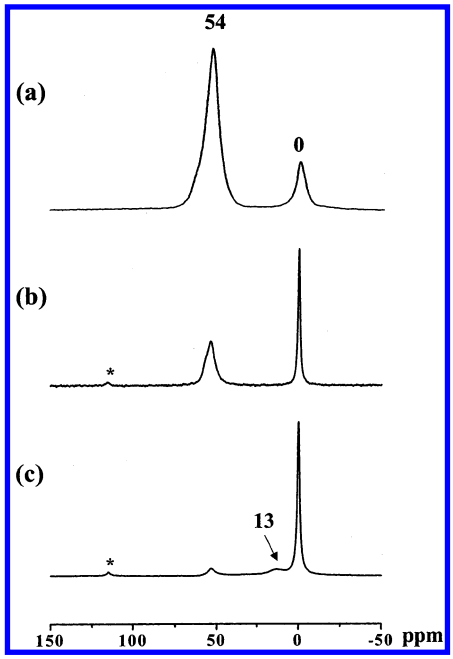

Figure 1. ^{27}Al MAS NMR spectra of (a) H-β, (b) H-β/AHFS-1.0-NH_4OAc, and (c) H-β/AHFS-1.6-NH_4OAc, acquired at spinning speeds of (a) 12 kHz, (b) and (c) 7 kHz. Both samples (b) and (c) are partially hydrated. Asterisks denote spinning sidebands. The spectra are not normalized.

experimental details and its applications has been given in earlier publications.[20,21] A spin−echo pulse was applied to the ^{19}F channel with and without simultaneous ^{27}Al irradiation during the evolution time (τ), the latter experiment serving as a control to eliminate spin−spin relaxation (T_2) effects. Refocusing of ^{19}F spins at the rotor echo, which are dipolar coupled to ^{27}Al spins, is prevented by the combination of MAS and continuous irradiation of the ^{27}Al nuclei. This results in a loss of ^{19}F spin intensity at the spin−echo. The ^{19}F{^{27}Al} TRAPDOR NMR experiments were performed at close to on-resonance irradiation conditions, with an ^{27}Al r.f. field amplitude of 50 kHz.

Results and Discussion

^{27}Al MAS NMR has been established as an efficient probe to determine the coordination and the local structure of specific aluminum species in zeolites since both tetrahedral and octahedral ^{27}Al sites can be readily resolved based on their distinctly different chemical shifts. Thus, the position of ^{27}Al resonance gives a good indication of the local environment of the aluminum site. For example, when the aluminum atoms are tetrahedrally coordinated to the framework, then a resonance in the range of 50−60 ppm is visible in the ^{27}Al NMR spectrum. EFAl species are usually octahedrally coordinated, and the responding signal has a chemical shift at around 0 ppm. The disadvantage of the ^{27}Al MAS NMR method is that a substantial number of the Al atoms may be "invisible", especially in a fully dehydrated zeolite sample, because of a large quadrupolar interaction with the electric field gradient at the ^{27}Al nucleus spin that is sited in a distorted environment. Therefore, the ^{27}Al MAS NMR measurements were performed after the samples were exposed to atmospheric moisture for various degrees of hydration.

^{27}Al MAS NMR of H-β/AHFS-x-NH_4OAc. The ^{27}Al MAS NMR spectra of H-β, and those after treatments by AHFS in the presence of NH_4OAc, are shown in Figure 1. The ^{27}Al MAS NMR spectrum of H-β reveals two resonances, one at 54 ppm attributable to the tetrahedral aluminum environment and the other at 0 ppm due to aluminum in the octahedral environment (Figure 1a). The resonance at 54 ppm due to the framework aluminum exhibits a shoulder near 57 ppm, suggesting the presence of two different crystallographic ^{27}Al sites in the framework of H-β zeolite, which have been observed with ^{27}Al MQMAS NMR.[15] With addition of AHFS ($x = 1.0$, Figure 1b), a significant decrease in the intensity of the resonance at 54 ppm accompanied by the appearance of a sharp peak at 0 ppm was observed, indicating that framework aluminum was expelled from the framework. The resonance at 0 ppm is due to octahedrally coordinated Al. Following the standard AHFS treatment, i.e., the dealuminated samples was further washed with hot water, the peak due to octahedrally coordinated Al disappeared and only tetrahedral coordinated Al existed. This implies that these octahedral Al species are EFAl species. With increasing AHFS content ($x = 1.6$), a new broad resonance at around 13 ppm due to aluminum in the octahedral environment was also observed (Figure 1c). It has been known that the line width of ^{27}Al NMR signals is very sensitive to the coordination environment around the aluminum atom. The narrow line width of the resonance at 0 ppm suggests that the EFAl species exhibits a very symmetrical environment. On the contrary, the larger line width for the resonance at 13 ppm implies a stronger quadrupolar interaction at this aluminum site, and thus a more distorted environment. It is also possible that the broad peak at 13 ppm is a result of a distribution of different EFAl species with similar chemical shifts. No new spectral feature was observed with higher AHFS contents. The peak at 54 ppm ascribed to framework tetrahedral aluminum decreases progressively with increasing amounts of AHFS, while the peak at 13 and 0 ppm increases as a consequence of the formation of more EFAl species. As evidenced in the ^{27}Al MAS NMR spectra shown in Figure 1, two different types of EFAl species resonating at 13 and 0 ppm were present in H-β/AHFS-x-NH_4OAc samples.

^{27}Al MAS NMR of H-β/AHFS-x-None. Figure 2 shows the ^{27}Al MAS NMR spectra of AHFS-treated H-β in the absence of NH_4OAc as a function of AHFS content. As compared to ^{27}Al spectra shown in Figure 1, the AHFS treatment in the absence of NH_4OAc significantly affects the ^{27}Al distribution. At a low level of AHFS ($x = 0.5$), besides framework aluminum at 54 ppm, a broad peak centered at around 13 ppm was observed (Figure 2a). In the case of H-β/AHFS-1.0-None sample (Figure 2b); however, an additional sharp peak at 0 ppm appeared. Further increasing the amount of AHFS ($x = 1.6$) resulted in the formation of a much broader pattern spread from-20 to −90 ppm (Figure 2c). The pattern spread from −20 to −90 ppm, which is induced by the second-order quadrupolar interaction, must be associated with an aluminum site with large quadrupolar interaction. Note that the upfield side of the pattern overlapped with the first-order sideband of the peak at 54 ppm. This pattern does not change upon further hydration. By assuming that there is no distribution for this site, a simulation of its line shape readily yields NMR parameters: isotropic chemical $\delta_{iso} = -5\pm2$ ppm, QCC = 9.5±0.3, and $\eta = 0.1\pm0.1$. The simulated spectrum is shown as dashed line in the inset of Figure 2c. This isotropic chemical shift is intermediate between those of AlO_6 and AlF_6 local environments. The large QCC for this EFAl species is indicative of a more distorted aluminum environment. To the best of our knowledge, this type of EFAl species was observed for the first time in dealuminated zeolites. Interestingly it is this kind of treatment, i.e., AHFS treatment in the absence of NH_4OAc, which leads to the formation of

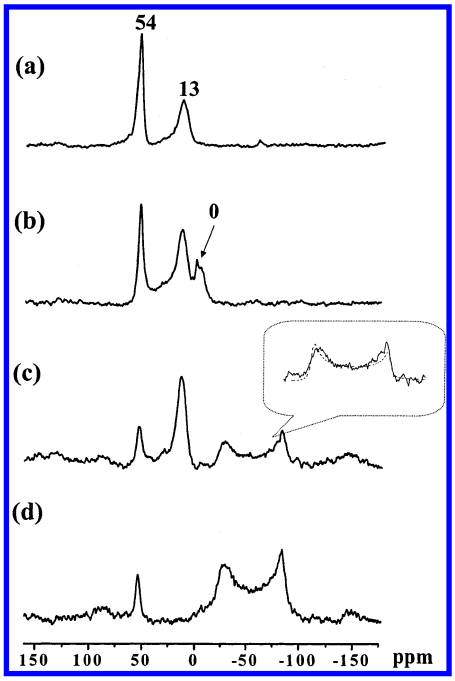

Figure 2. ^{27}Al MAS NMR spectra of H-β/AHFS-x-None, where x = (a) 0.5, (b) 1.0, (c) 1.6, and (d) 3.2, acquired at spinning speeds of (a) 7 kHz and others at 12 kHz. All the samples are partially hydrated except (d), which is fully hydrated. Asterisks denote spinning sidebands. The spectra are not normalized.

such EFAl species. The resonance at 13 ppm was no longer observed and the pattern spread from −20 to −90 ppm dominated the spectrum as higher amount of AHFS was added (Figure 2d). As evidenced in Figure 2, there are three different types of EFAl, namely the resonances at 13 ppm, 0 ppm, and the pattern spread from −20 to −90 ppm, present in the AHFS-treated H-β in which no NH_4OAc was added. The ^{27}Al NMR results demonstrated that the experimental conditions of AHFS dealumination, that is, in the presence and absence of NH_4OAc in this case, strongly affect the amount, state, and nature of EFAl species as demonstrated in Figures 1 and 2.

The Effect of Hydration Level on the ^{27}Al Spectrum. To investigate the hydration level on the state of EFAl species, dealuminated samples were exposed to atmospheric moisture for different periods of time. When the H-β/AHFS-1.6-NH_4OAc sample was analyzed after prolonged exposure to atmospheric moisture, the peak at 13 ppm disappeared, and the sharp peak at 0 ppm seemed to be superposed by a broad signal at the same peak position (Figure 3a, right). For partially hydrated H-β/AHF-3.2-None sample (Figure 3b, left), a broad peak at around 32 ppm was observed. It has been demonstrated that a five-coordinated aluminum[22] or a distorted tetrahedral aluminum[23] gives a distinct signal between those corresponding to a four- and a six-coordinated aluminum. Therefore, the peak at 32 ppm is related to Al species in an intermediate, extraframework environment between the framework tetrahedral Al and the extraframework octahedral Al. After the sample was further hydrated for one more week, the bump at around 32 ppm disappeared, and a powder pattern spread in the range of −20 to −90 ppm was observed (Figure 3b, right). This change has to be associated with the hydration level of the sample. Upon hydration, the nature and status of EFAl species is evidently altered.

The Degree of Dealumination. As demonstrated, quantification of the total Al content in these dealuminated samples was complicated by the moisture content and compositional changes during the treatments. Some errors might occur because of the loss of some water-soluble aluminum fluorides during filtration. Furthermore, the quadrupolar effects of the aluminum nuclei should also be taken into account. In the case of dealumination with a total amount of AHFS, which corresponds to 100% of total aluminum content of H-β, resulted only in approximately 47% and 65% dealumination for H-β/AHFS-1.0-NH_4OAc and H-β/AHFS-1.0-None, respectively. Extensive treatment with an excess of AHFS resulted in a further dealumination up to ∼96% for both treatments. In a previous work on the dealumination of ZSM-5 and Y zeolites in the presence of NH_4OAc, AHFS removed only 24% and 50% framework aluminum atoms if a total amount of AHFS corresponding to 100% of its framework aluminum atoms was used.[24]

^{27}Al{^{19}F} REDOR NMR. Although REDOR NMR was originally designed to measure heteronuclear dipolar coupling, and thus internuclear distance,[16] here it was used only to qualitatively provide the information of correlation between ^{19}F and ^{27}Al nuclei due to the complexity of the dealuminated sample. Typical ^{27}Al{^{19}F} REDOR NMR spectra are shown in Figure 4. The reduction in the intensity of the ^{27}Al due to ^{19}F dephasing is shown in Figure 4c. A significant loss in ^{27}Al intensity (6%), comparable to the REDOR fraction calculated for a static Al−F bond (1.8−2.2 Å) observed for the peak at 0 ppm suggests that the aluminum in this EFAl species is directly bonded to fluorine. It is also interesting to note that two peaks for framework Al can be resolved in the difference spectrum of ^{27}Al{^{19}F} REDOR NMR experiments, consistent with the observation with MQMAS NMR studies.[15] Similar experiments performed on the H-β/AHFS-x-None samples also show that the peak at 13 ppm and the pattern spread from −20 to −90 ppm exhibit significant REDOR effects, indicating these EFAl species contain Al−F bonds.

^{19}F NMR of Aqueous AHFS Solution. AHFS is very soluble in water,

$$(NH_4)_2SiF_6 \leftrightarrow 2NH_4^+ + SiF_6^{2-} \quad (1)$$

and SiF_6^{2-} undergoes hydrolysis as follows:

$$SiF_6^{2-} + 4H_2O \leftrightarrow Si(OH)_4 + 6F^- + 4H^+ \ (K\sim 10^{30}) \quad (2)$$

The reaction in eq 2 is strongly shifted to the right when pH becomes higher than 6−7. Thus, AHFS can be used as the source for silicon and fluoride.[25] ^{19}F solution NMR provides a simple way to determine the composition of AHFS in the presence and absence of NH_4OAc (i.e., pH), which would be helpful to assign the ^{19}F NMR peaks in the dealuminated zeolite samples.

Figure 5 illustrates the effect of increasing pH on the ^{19}F spectrum of aqueous AHFS solution. A single peak at −130 ppm due to SiF_6^{2-} was observed for aqueous 0.4 M AHFS solution (Figure 5a). With addition of NH_4OAc, a new peak appeared at −116 ppm (Figure 5b), which can be ascribed to free F^- corresponding to the peak observed for aqueous NH_4F solution. As seen in Figure 5b−d, the intensity ratio of SiF_6^{2-} to F^- depends on the pH of the solution, decreasing from 1.3 to 0.2 as the pH of the solution increases from 6.7 to 6.9. When the pH is higher than 7, the peak at −130 ppm due to SiF_6^{2-} disappears and only free F^- at −116 ppm is observed, confirming that the reaction in eq 2 strongly shifts to the right.

^{19}F MAS NMR of H-β/AHFS-x-NH_4OAc. A better understanding of the nature of the fluorinated species formed during the dealumination process can be gained through ^{19}F MAS NMR spectroscopy. To avoid possible strong homonuclear ^{19}F−^{19}F

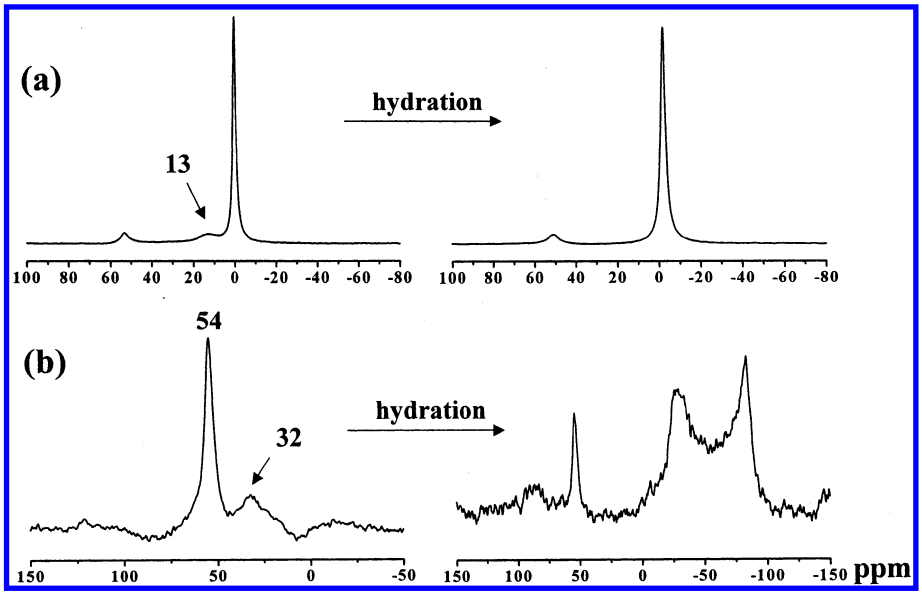

Figure 3. ^{27}Al MAS NMR spectra of partially (left) and fully hydrated (right) samples: (a) H-β/AHFS-1.6-NH_4OAc and (b) H-β/AHFS-3.2-None.

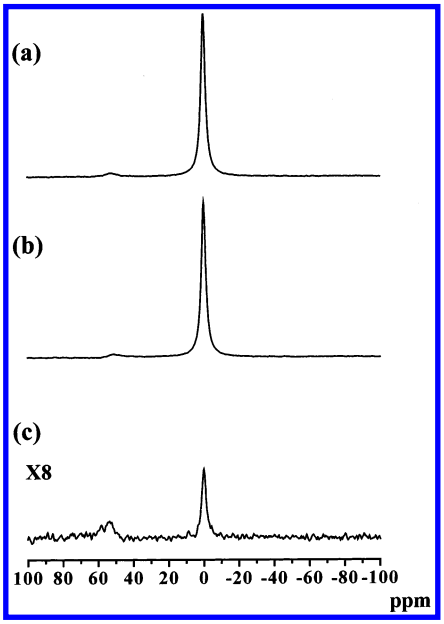

Figure 4. ^{27}Al{^{19}F} REDOR NMR spectra of H-β/AHFS-1.0-NH_4OAc acquired (a) without and (b) with applying ^{19}F π pulses (total dephasing time = 160 μs). The difference spectrum is shown in (c).

couplings experiencing in fluorinated species, ^{19}F MAS NMR experiments were performed on partially dehydrated samples, which were obtained by thermal treatment of the dealuminated samples at 60 °C overnight. The fully dehydrated samples, obtained by calcination of samples under vacuum at 400 °C, would be expected to experience stronger dipolar interactions. Figure 6 shows the ^{19}F MAS NMR spectra of H-β/AHFS-x-NH_4OAc as a function of AHFS content. At low level of AHFS (x = 0.5), three major peaks at −143, −158, and −173 ppm and three small peaks at −130, −125, and −183 ppm were observed. The peak at −130 ppm can be assigned to unreacted SiF_6^{2-}, and the peak at −125 ppm is presumably due to the presence of the F^- counterion of NH_4^+ or H^+ occurring in channels.[26] The peak at −143 ppm dominated the spectrum whereas a broad, less intense peak centered at −156 ppm was observed as the amount of AHFS was further increased (Figure 6b and 6c). Since the major EFAl species observable in the corresponding ^{27}Al spectrum is at 0 ppm, the peak at −143 ppm in the ^{19}F spectrum must be associated with this EFAl species.

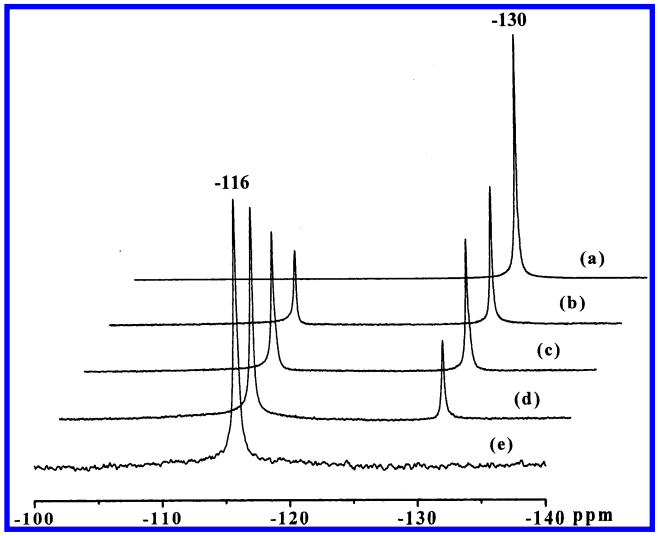

Figure 5. The pH effects on the ^{19}F solution NMR spectra of aqueous AHFS solution in the presence of NH_4OAc, (a) aqueous AHFS solution (0.4 M), pH = 3.5, (b) pH = 6.7, (c) pH = 6.8, (d) pH = 6.9, and (e) pH = 7.1.

The peaks at −143 ppm can be assigned to $(NH_4)_3AlF_6$. The assignment is supported by the inspection of the spectra recorded for the position of ^{19}F resonance line in $(NH_4)_3AlF_6$ (−143 ppm). The presence of $(NH_4)_3AlF_6$ is also confirmed by X-ray diffraction studies, which shows small additional peaks at 2θ = 17° and 20° that are identical with the typical pattern of $(NH_4)_3AlF_6$. On the other hand, the broad resonance due to EFAl species, which was observed at 13 ppm in the ^{27}Al spectrum, corresponds to the broad ^{19}F resonance centered at 156 ppm. According to the literature,[27] the chemical shifts of the larger resonances at −173 and −183 ppm are ascribed to hydrated and dehydrated AlF_3 phases, respectively, and are indicative of Al−F−Al linkages. By washing the dealuminated samples with hot water, all the ^{19}F signal intensities decrease dramatically, which support the assignments of the above ^{19}F-containing species are not in the framework.

^{19}F MAS NMR of H-β/AHFS-x-None. The ^{19}F MAS NMR spectra of H-β/AHFS-x-None are displayed in Figure 7. Unlike the H-β/AHFS-x-NH_4OAc samples, the peak at −143 ppm was not observed for H-β/AHFS-0.5-None (Figure 7a). On the other hand, the peak centered at around −158 ppm dominated the

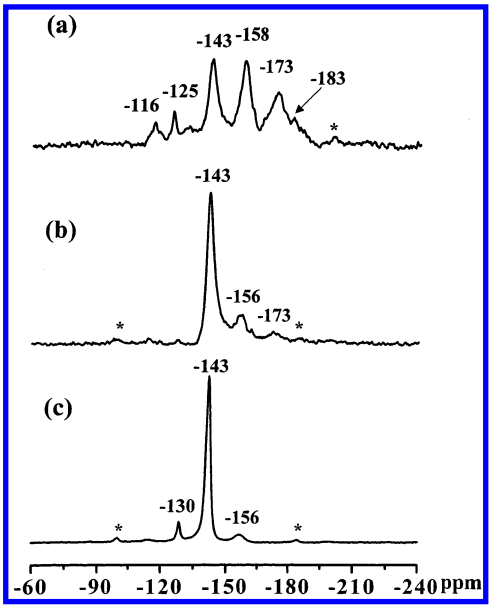

Figure 6. ^{19}F MAS NMR spectra of H-β/AHFS-x-NH_4OAc, where x = (a) 0.5, (b) 1.0, (c) 3.2. Asterisks denote spinning sidebands.

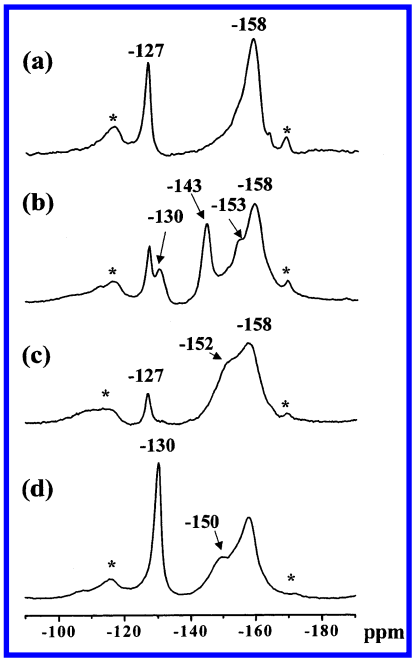

Figure 7. ^{19}F MAS NMR spectra of H-β/AHFS-x-None, where x = (a) 0.5, (b) 1.0, (c) 1.6, and (d) 3.2. Asterisks denote spinning sidebands.

spectrum. Much more of the unreacted fluorides at −127 and −130 ppm remained in the zeolite pore as compared to the case of adding NH_4OAc. With increasing AHFS content to $x = 1.0$, the peak at −143 ppm and a shoulder at −153 ppm were observed, indicating that a variety of fluoride species was formed. Further increasing AHFS content to $x = 1.6$, the peak at −143 ppm no longer existed, and the shoulder slightly shifted to −152 ppm and became broader (Figure 7c). At higher AHFS content the peak at −153 ppm disappeared, and the peak centered at −150 ppm became evident (Figure 7d). The resonances at −153 and −150 ppm should be consistent with what observed in the corresponding ^{27}Al spectra. When AHFS content increased from 1.6 to 3.2, the ^{27}Al resonance at 13 ppm disappeared, and the ^{27}Al resonance spread from −20 to −90 ppm dominated the spectrum, corresponding to the ^{19}F peak shift from −153 ppm to −150 ppm. Thus the ^{19}F resonances at −153 and −150 ppm relate to the ^{27}Al resonance at 13 ppm and that spread from −20 to −90 ppm, respectively.

To further identify the ^{19}F resonances observed for dealuminated zeolites, purely siliceous MCM-41 treated with AHFS was also studied for comparison. A major peak at −158 ppm was observed for AHFS-treated MCM-41 in the absence of NH_4OAc (not shown). Since there is no aluminum present in MCM-41, the peak at −158 ppm must be related to Si−F groups, resulting from the replacement of hydroxyl group in the silanols by fluorine atom, or a terminal fluorine atom at the surface. This implies that fluorination with AHFS resulting in the formation of (SiO_3)Si−F groups, where −F has replaced −OH, cannot be entirely excluded. Therefore, the peak at −158 ppm observed in H-β/AHFS-0.5-NH_4OAc sample (Figure 6a) can be assigned to Si−F groups. Unfortunately, this signal may be overlapped with those of aluminum fluoro-complexes, and results in a broad signal centered at −156 ppm at higher AHFS content. Thus the quantitative distinction between the fluorine atom in Si−F groups and the aluminum fluoro-complexes is difficult.

^{19}F{^{27}Al} TRAPDOR NMR of AHFS-Treated H-β. ^{19}F{^{27}Al} TRAPDOR NMR experiments were performed to determine the connectivity of fluorine with aluminum. In the ^{19}F{^{27}Al} TRAPDOR NMR experiments, the ^{19}F signal intensities of fluorinated species that are nearby ^{27}Al spins are expected to decrease in the spectrum acquired with ^{27}Al irradiation. This occurs because the dephasing during τ of the spin−echo experiment, due to ^{19}F−^{27}Al dipolar coupling, is no longer refocused on applying ^{27}Al irradiation.[17] Thus, the signal of fluorinated species that are strongly coupled to aluminum atoms will be significantly suppressed. On the other hand, those fluorinated species that are not coupled to ^{27}Al spins will be unaffected upon ^{27}Al irradiation. The only fluorinated species observed in the difference spectrum are those close to aluminum atoms. Hence, ^{19}F{^{27}Al} TRAPDOR NMR can be used to establish the connection between ^{19}F and ^{27}Al nuclei.

The ^{19}F reference spectrum, which is analogous to a Hahn echo experiment (i.e., no ^{27}Al irradiation), of H-β/AHFS-1.0-None sample is shown in Figure 8a, consisting of the peak at −143 ppm and the broad resonance in the range of −150 to −158 ppm. On-resonance ^{27}Al irradiation for one rotor period ($\tau = 80\ \mu$s) results in a loss of all the intensities of resonances as shown in Figure 8b. As seen in the difference spectrum (Figure 8c), ^{19}F{^{27}Al} TRAPDOR effects were observed for these resonances, indicating that all these species are in close proximity to aluminum atoms. The smaller TRAPDOR effect observed for the peak at −143 ppm implies that fast rotation of the AlF_6^{3-} ions cancels the ^{19}F−^{27}Al dipolar interaction.

It is noticed that both peaks at −127 ppm and −130 ppm exhibit small TRAPDOR effects. The peak at −127 ppm is assigned to the F^- ion-paired with NH_4^+/H^+ occurring in the channels. Since NH_4^+/H^+ ions are associated with aluminum atoms to balance the charge of zeolite framework, a small TRAPDOR effect due to the peak at −127 ppm is possible. Considering the complexity of the studied system the SiF_6^{2-} ion (at −130 ppm) might also exhibit a small TRAPDOR effect due to nearby extraframework Al species. Nevertheless, we cannot totally exclude the possibility that these effects are due to incompletely corrected echo dephasing caused by the ^{27}Al irradiation.

Nature of the Fluorinated Species. Utilizing the above NMR results, a better understanding regarding the formation of aluminum fluoro-complexes occurring in the dealuminated H-β as a function of AHFS content can be detailed. For H-β/AHFS-

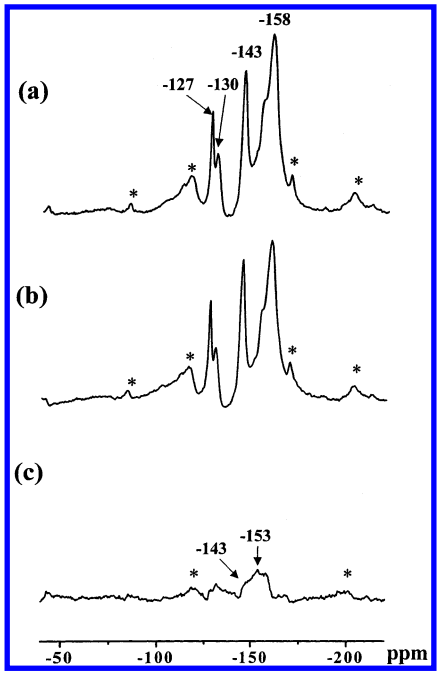

Figure 8. $^{19}F\{^{27}Al\}$ TRAPDOR NMR spectra of H-β/AHFS-1.0-None, (a) without and (b) with ^{27}Al irradiation. The difference spectrum is shown in (c). Asterisks denote spinning sidebands.

1.0-NH_4OAc, the major ^{19}F resonance at -143 ppm corresponds to the dominant EFAl species resonating at 0 ppm in the ^{27}Al spectrum (cf. Figure 1b and 6b), which can be assigned to $(NH_4)_3AlF_6$. The assignment is consistent with the ^{27}Al and ^{19}F chemical shifts for crystalline $(NH_4)_3AlF_6$. In addition, the ^{27}Al narrow line width indicates that this aluminum species is in a very symmetrical octahedral environment. Evidence of the formation of $(NH_4)_3AlF_6$ was reported by Kowalak[28] who suggested this compound to be formed by the following reaction:

$$Al^{3+} + 6NH_4^+ + 6F^- \rightarrow (NH_4)_3AlF_6 + 3NH_3 + 3H^+ \quad (3)$$

After treatment using a high concentration of AHFS ($x = 1.0$), besides the peak at -143 ppm a broad signal centered at -156 ppm (Figure 6b) and a shoulder at -153 ppm (Figure 7b) were observed. The peaks at -153 and -156 ppm correspond to the broad ^{27}Al resonance at 13 ppm. On the basis of its larger line width as compared to that of the resonance at 0 ppm, it implies that the corresponding aluminum fluoro-complexes at -153 and -156 ppm in the ^{19}F spectrum exhibit a distribution of different aluminum fluorides. The ^{27}Al resonance at 13 ppm, corresponding to the ^{19}F resonances in the range of -153 to -156 ppm, can be attributed to $[AlF_x(H_2O)_{6-x}]^{3-x}$ (most likely $x = 1$ or 2).

The absence of ^{27}Al resonance at 0 ppm and ^{19}F resonance at -143 ppm for H-β/AHFS-0.5-None suggests that the formation of $(NH_4)_3AlF_6$ does not occur at low concentration of AHFS in the absence of NH_4OAc. It is interesting to note that, however, the $(NH_4)_3AlF_6$ species was formed only in the case of H-β/AHFS-1.0-None sample. At higher AHFS content, the ^{27}Al resonances at 13 ppm, and the pattern spread in the range of -20 to -90 ppm were associated with the ^{19}F resonances at -153 and -150 ppm, respectively (Figure 2 and Figure 7). Hence, ^{27}Al MAS NMR results of AHFS-treated H-β in the absence of NH_4OAc indicated that the incorporation of fluorine atoms into H-β zeolites resulted in the formation of two major ^{27}Al sites: 13 ppm, and the pattern spread from -20 to -90 ppm. The latter resulted from the intermediate, extraframework ^{27}Al resonance at 32 ppm (Figure 3b, left). The ^{27}Al resonance at 32 ppm might initially consist of five coordinated AlF_xO_{5-x} species and then became $AlF_xO_{5-x}(H_2O)$, an octahedral Al species after hydration. The ^{19}F resonances can be compared with those obtained for complexes in solution. Sur and Bryant[29] have studied fluoroaluminum complexes in solution and adsorbed by zeolites. They have assigned sharp lines from -145 to -156 ppm to complexes such as $[AlF_x(H_2O)_{6-x}]^{3-x}$, as found in other studies on aqueous solutions.[30] The more positive the complex, the more upfield is the shift. In fluorinated alumina, Fischer and co-workers[31] have observed broad but resolved lines at -154 and -143 ppm that they assigned to $(Al^{VI}O_5F)$ and $(Al^{VI}O_4F_2)$ environments. In the present study, two types of aluminum fluoro-complexes have to be considered, i.e., $AlF_x(OH)_{3-x(aq)}$ and $[AlF_x(H_2O)_{6-x}]^{3-x}$ ($x = 1-3$). If the ratio of F/Al is constant, the ^{19}F shift of $AlF_x(OH)_{3-x(aq)}$ would become more positive as compared with that of $[AlF_x(H_2O)_{6-x}]^{3-x}$. Considering the relatively close chemical shift observed for a pseudo-octahedral Al^{3+} in hydrated forms of AlF_3 (at 20 ppm),[32] we assign the ^{27}Al resonance at 13 ppm to $[AlF_x(H_2O)_{6-x}]^{3-x}$ species, which results from the substitution by fluorine of water molecules in the coordination sphere of octahedral aluminum atoms. The observation for the resonance shifting to 0 ppm after rehydration supports the assignment. On the other hand, the ^{27}Al resonance spread from -20 to -90 ppm having a larger quadrupolar coupling can be attributable to aluminum hydroxy-fluorides, i.e., $AlF_x(OH)_{3-x(aq)}$, which are formed from the substitution by fluorine of water molecules in the coordination sphere of octahedral Al$-$OH groups. One might expect that $AlF_x(OH)_{3-x(aq)}$ species exhibit more distorted environments as compared to $[AlF_x(H_2O)_{6-x}]^{3-x}$ species, and thus experience a stronger quadrupolar coupling. Moreover, a significant amount of Al$-$OH present in zeolite H-β has been identified with $^1H\{^{27}Al\}$ TRAPDOR NMR experiments in our earlier study.[33] Our preliminary results for the AHFS-treated H-mordenite samples (Si/Al = 10) in the absence of NH_4OAc show that only two resonances at 13 and 0 ppm were observed in the ^{27}Al spectrum, and the pattern spread from -20 to -90 ppm was not detected. Since there is a negligible amount of Al$-$OH groups present in H-mordenite, as confirmed by $^1H\{^{27}Al\}$ TRAPDOR NMR,[33] this provides an additional indirect support that the pattern spread from -20 to -90 ppm observed for H-β has to be related with Al$-$OH groups. Martinez et al.[30] reported that the ^{19}F chemical shifts for $[AlF_x(H_2O)_{6-x}]^{3-x}$ and $AlF_x(OH)_{3-x(aq)}$ in the solution are in a similar range of -152 to -156 ppm; the latter species has a relatively downfield shift. Even if the rigorous assignment of these two types of fluoro-aluminate complexes seems difficult, as deduced from their similar ^{19}F chemical shifts, discrimination between these different species is feasible by monitoring the change of ^{19}F peak shift as a function of AHFS content. Furthermore, there are significant differences in their ^{27}Al chemical shifts and spectral line shapes despite the geometry of all these complexes corresponding to a hexacoordination. Thus, we assign the ^{19}F resonances in the range of -153 to -156 ppm to $[AlF_x(H_2O)_{6-x}]^{3-x}$ and the ^{19}F resonance at -150 ppm to $AlF_x(OH)_{3-x(aq)}$, respectively. The ^{19}F peak assignments for different fluorinated species are summarized in Table 1.

Possible Mechanisms of Dealumination. Clear differences appeared in the formation of aluminum fluoro-complexes as a result of the dealumination procedure. Combined with the ^{19}F and ^{27}Al NMR observations in this study, these differences may be better understood in terms of the dealumination mechanisms that have been proposed. The proposed mechanisms of the AHFS dealumination in the literature basically involves two

TABLE 1: ^{19}F Peak Assignments for Fluorinated Species in AHFS-Treated H-β Samples

^{19}F chemical shift	assignment
−127 ppm	F^- ion paired with NH_4^+/H^+
−130 ppm	SiF_6^{2-}
−143 ppm	$(NH_4)_3AlF_6$
−150 ppm	$AlF_x(OH)_{3-x(aq)}$
−152 to −156 ppm	$[AlF_x(H_2O)_{6-x}]^{3-x}$
−158 ppm	Si−F
−173 ppm	AlF_3 (hydrated)
−183 ppm	AlF_3 (dehydrated)

steps.[8] During AHFS dealumination in the presence of NH_4OAc, aluminum is first extracted from the framework leaving a vacancy in which silicon is inserted in a second step. It has been suggested that aluminum is removed in the form of AlF_6^{3-} ions whereas the inserted species is monomolecular silicic acid $Si(OH)_4$.[12] Our ^{19}F and ^{27}Al NMR results showed that most of the extracted Al^{3+} ions readily reacted with F^-, and resulted in the formation of $(NH_4)_3AlF_6$ species that were evident from the signals at 0 ppm in the ^{27}Al spectrum and −143 ppm in the ^{19}F spectrum, respectively. XRD results also confirmed the presence of $(NH_4)_3AlF_6$. The formation of AlF_3 phases was also verified by the observation of the ^{19}F resonance at 173 and 183 ppm for treatments at low AHFS content (Figure 6a). Some variants of a $[AlF_x(H_2O)_{6-x}]^{3-x}$ species formed from aqueous solution of AlF_3,[34] would be expected to give to another type of octahedral Al^{3+} in the ^{27}Al spectrum. Indeed, another ^{27}Al resonance at 13 ppm has been observed which was accounted for this aluminum fluoro-complex (Figure 1c). Upon further hydration, this resonance disappeared and the intensity of the resonance at 0 ppm was enhanced probably due to the transformation of $[AlF_x(H_2O)_{6-x}]^{3-x}$ species into $Al(H_2O)_6^{3+}$. At a high level of AHFS while the concentration of fluoride ion is sufficiently enough, the dominant EFAl species became $(NH_4)_3AlF_6$. Thus, it is concluded that the essential part of the dealumination process carried on with AHFS in the presence of NH_4OAc is that the extracted Al^{3+} reacts with F^- to form AlF_3 and $(NH_4)_3AlF_6^{3-}$ species. Previous studies have shown that different aluminum fluoride species such as $[AlF_x(H_2O)_{6-x}]^{3-x}$ ($x = 1-5$) were formed successively as the concentration of fluoride ion increased. At sufficiently high fluoride ion concentration, an octahedral AlF_6^{3-} species started to form in appreciable amount,[28] consistent with our observations.

In the case of without adding NH_4OAc, the zeolite solution was acidic (pH ∼ 3.5). Under such conditions, the zeolite sample was dealuminated by acid leaching induced by AHFS, and thus resulted in the formation of significant amounts of terminal silanols and EFAl species. The true nature of EFAl is not known even though studies employing different physical methods have been made.[35−37] Several forms of EFAl have been proposed in the literature, such as boehmite,[38,39] psuedo-boehmite, $Al(OH)_3$, $Al(OH)^{2+}$, and AlO^+ or some polymeric aluminum species.[40] Recently Apelian et al. proposed that the acid leaching of zeolites results in the formation of $Al(OH)_2^+$.[4] In parallel with dealumination, SiF_6^{2-} serves as a fluorination reagent, and the resulting fluoride ions react with both terminal silanols and Al−OH moieties of intermediate (transient) products leaving the framework, which are especially abundant in H-β as confirmed by ^{1}H{^{27}Al} TRAPDOR NMR in our earlier study,[32] to form Si−F groups and aluminum hydroxyfluorides. On the basis of the fact that zeolite β is easier to dealuminate than the other zeolite types (mordenite, ZSM-5, and ferrierite),[41] it seems probable that the first step in H-β is that fluoride ions react with Si−OH groups at low AHFS content, and EFAl species, created by the calcinations and acid leaching, are then fluorinated with increasing AHFS content. Clearly, the dealumination of H-β leading to the formation of $(NH_4)_3AlF_6$ does not become energetically favorable in the absence of NH_4OAc. On the contrary, fluorination of both the silanols at the surface and EFAl species proceed predominantly.

On the basis of the ^{27}Al and ^{19}F NMR experimental results, some possible reaction pathways for AHFS dealumination process are proposed as illustrated in Scheme 1. (Note that eqs 5 and 7 are not balanced.)

SCHEME 1: Possible Reaction Pathways for AHFS-Treated H-β in the Presence and Absence of NH_4OAc

(a) in the presence of NH_4OAc

$$Al^{3+} + 6NH_4^+ + 6F^- \rightarrow (NH_4)_3AlF_6 + 3NH_3 + 3H^+ \quad (3)$$

$$Al^{3+} + 3F^- + nH_2O \rightarrow AlF_3 \cdot nH_2O\ (n = 1-3) \quad (4)$$

$$AlF_3 + H_2O \rightarrow [AlF_x(H_2O)_{6-x}]^{3-x} \quad (5)$$

(b) in the absence of NH_4OAc

$$AlF_3 + H_2O \rightarrow [AlF_x(H_2O)_{6-x}]^{3-x} \quad (5)$$

$$Si-OH + F^- \rightarrow Si-F + OH^- \quad (6)$$

$$\{Al(OH)_3, Al(OH)_2^+, Al(OH)^{2+}\} + F^- \rightarrow AlF_x(OH)_{3-x} \quad (7)$$

In the presence of NH_4OAc, the concentration of fluoride ion in the solution is sufficient, according to eq 2, to favor the formation of fluorinated aluminum species depicted in eqs 3−5 of Scheme 1. It is clear that the control of pH to be near neutral is a key step responsible for the strong preference for the formation of AlF_6^{3-}. In the absence of NH_4OAc, on the contrary, the solution is too acidic to provide enough concentration of fluoride ion to form AlF_6^{3-} (see Figure 5). Therefore, the reaction pathways depicted in eqs 5−7 of Scheme 1 become dominant. Our ^{27}Al and ^{19}F NMR data suggest that a variety of aluminum fluorides can result from reaction pathways depicted in eqs 3−7, and the fluoride content in the solution seems to be important in determining which pathway predominates. The reaction of fluoride ions with the aluminum ion and consequently the formation of various fluoroaluminates strongly depend on the fluoride ion concentration and the type of EFAl species.

Conclusions

This work has shown that fluorinated EFAl species in H-β can be produced in different forms, depending on the preparation history of the catalyst. After AHFS dealumination, EFAl species were predominantly created in octahedral form. By controlling the pH of the zeolite solution with NH_4OAc, most of the extracted Al^{3+} ions react with F^-, formed by hydrolysis of SiF_6^{2-}, and predominantly result in the formation of $(NH_4)_3AlF_6$. The control of pH to be near neutral is a key step responsible for the strong preference for the formation of AlF_6^{3-}. In the absence of NH_4OAc, on the other hand, the acid leaching induced by AHFS created more Si−F groups and EFAl species. In parallel with dealumination, AHFS served as a fluorination reagent, and reacted with both the terminal Si−OH groups and EFAl species to form Si−F groups and a variety of aluminum

fluoro-complexes including $[AlF_x(H_2O)_{6-x}]^{3-x}$ and $AlF_x(OH)_{3-x(aq)}$. Complementary characterization with ^{19}F and ^{27}Al MAS NMR allows the detection of different aluminum fluoro-complexes formed during the AHFS dealumination process, and thus provides a better insight into the dealumination mechanism.

Acknowledgment. We thank the National Science Council of Taiwan for financial support and Ms. R.-R. Wu at National Cheng Kung University for some NMR measurements.

References and Notes

(1) Chen, N. Y.; Garwood, W. E.; Dwyer, F. G. *Shape Selective Catalysis in Industrial Applications*, 2nd ed.; Dekker: New York, 1996.
(2) Parikh, P. A.; Subrahmanyam, N.; Bhat, Y. S.; Halgeri, A. B. *J. Mol. Catal.* **1994**, *88*, 85.
(3) Maache, M.; Janin, A.; Lavalley, J. C.; Joly, J. F. *Zeolites* **1993**, *13*, 419.
(4) Apellian, M. R.; Fung, A. S.; Kennedy, G. J.; Degnan, T. F. *J. Phys. Chem.* **1996**, *100*, 16577.
(5) Zaiku, X.; Qingling, C.; Chengfang, Z.; Jiaqing, B.; Yuhua, C. *J. Phys. Chem. B* **2000**, *104*, 2853.
(6) Weitkamp, J.; Sakuth, M.; Chen, C.; Ernst, S. *J. Am. Soc., Chem. Commun.* **1989**, 1908.
(7) Triantafillidis, C. S.; Vlessidis, A. G.; Nalbandian, L.; Evmiridis, N. P. *Microporous Mesoporous Mater.* **2001**, *47*, 369.
(8) Skeels, G. W.; Breck, D. W. In *Proceedings of the Sixth International Zeolite Conference*; Olson, D. H., Bisio, A., Eds.; Butterworths: Surrey, 1983; p 87.
(9) Breck, D. W.; Blass, H.; Skells, G. W. U.S. Patent 4503203, **1985**.
(10) Meier, W. M.; Olson, D. H. *Atlas of Zeolite Structure Types*, 3rd ed.; Butterworth-Heinemann: London, 1992; p 58.
(11) Bourgeat-Lami, E.; Massiani, P.; Di Renzo, F.; Espiau, P.; Fajula, F. *Appl. Catal.* **1991**, *72*, 139.
(12) Perez-Pariente, J.; Sanz, J.; Fornes, V.; Corma, A. *J. Catal.* **1990**, *124*, 217.
(13) Kircsi, I.; Flego, C.; Pazzuconi, G.; Parker, W. O.; Millini, R.; Perego, C.; Bellussi, G. *J. Phys. Chem.* **1994**, *98*, 4627.
(14) Corma, A.; Martinez, A.; Arroyo, P. A.; Monteiro, J. L. F.; Sousa-Agular, E. F. *Appl. Catal. A: Gen.* **1996**, *142*, 139.
(15) van Bolhoven, J. A.; Koningsberger, D. C.; Kunkeler, P.; van Bekkum, H.; Kentgens, A. P. *J. Am. Chem. Soc.* **2000**, *122*, 12842.
(16) Gullion, T.; Schaefer, J. *J. Magn. Reson.* **1989**, *81*, 196.
(17) Grey, C. P.; Vega A. *J. Am. Chem. Soc.* **1995**, *117*, 8232.
(18) Das, D.; Tsai, C.-M.; Cheng, S. *Chem. Commun.* **1999**, 473.
(19) Fenzke, D.; Freude, D.; Frohlich, T.; Haase, J. *Chem. Phys. Lett.* **1984**, *111*, 171.
(20) Kao, H.-M.; Grey, C. P. *Chem. Phys. Lett.* **1996**, *259*, 459.
(21) Kao, H.-M.; Grey, C. P. *J. Phys. Chem.* **1996**, *100*, 5105.
(22) Alemany, L. B.; Kirker, G. W. *J. Am. Chem. Soc.* **1986**, *108*, 6158. (b) Gilson, J. P.; Edwards, G. C.; Peters, A. W.; Rajgopalan, K.; Wormsbecher, R. F.; Roberie, T. G.; Shatlock, M. P. *J. Chem. Soc. Chem. Commun.* **1987**, 91.
(23) Samoson, A.; Lippmaa, E.; Engelhardt, G.; Lohse, U.; Jerschkewiz, H. G. *Chem. Phys. Lett.* **1987**, *134*, 589.
(24) Garralon, G.; Fornes, V.; Corma, A. *Zeolites* **1988**, *8*, 268.
(25) Voegtlin, A. C.; Ruch, F.; Guth, J. L.; Patarin, J.; Huve, L. *Microporous Mater.* **1997**, *9*, 95.
(26) Delmotte, L.; Soulard, M.; Guth, F.; Seive, A.; Lopez, A.; Guth, J. L. *Zeolites* **1990**, *10*, 778.
(27) Decanio, E. C.; Bruno, J. W.; Nero, V. P.; Edwards, J. C. *J. Catal.* **1993**, *140*, 84.
(28) Kowalak, S. *Acta Chim. Acad. Sci. Hung.* **1981**, *107*, 19.
(29) Sur, S. K.; Bryant, R. G. *Zeolites* **1996**, *16*, 118.
(30) Martinez, E. J.; Girardet, J.-L.; Morat, C. *Inorg. Chem.* **1996**, *35*, 706.
(31) Huggins, B. A.; Ellis, P. D. *J. Am. Chem. Soc.* **1992**, *114*, 2098.
(32) Fischer, L.; Harle V.; Kasztelan, S.; d′Espinose de la Caillerie, J. B. *Solid State Nucl. Magn. Reson.* **2000**, *16*, 85.
(33) Kao, H. M.; Yu, C. Y.; Yeh, M. C. *Microporous Mesoporous Mater.* **2002**, *53*, 1.
(34) Matwiyoff, N. A.; Wageman, W. E. *Inorg. Chem.* **1970**, *9*, 1031.
(35) Shannon, R. D.; Gardner, K. H.; Staley, R. H.; Bergeret, G.; Gallezot, P.; Guisnet, M. *J. Catal.* **1991**, *130*, 459.
(36) Anderson, M. W.; Klinowski, J. *Zeolites* **1986**, *6*, 455.
(37) van Niekerk, M. J.; Fletcher, C. Q. J.; O'Connor, C. T. *J. Catal.* **1992**, *138*, 150.
(38) Shannon, R. D.; Gardner, K. H.; Staley, R. H.; Bergeret, G.; Gallezot, P.; Auroux, A. *J. Phys. Chem.* **1985**, *89*, 4778.
(39) Kuhl, G. H. *Molecular Sieves*; Uytterhoeven, J. B., Ed.; Lueven University Press: Belgium, 1973; p227.
(40) Kuhl, G. H. *ACS Symp. Ser.* **1977**, *40*, 96.
(41) Müller, M.; Harvey, G.; Prins, R. *Microporous Mater.* **2000**, *34*, 281.